Available online at www.sciencedirect.com
ScienceDirect
European Journal of Medicinal Chemistry 43 (2008) 1696–1705
EUROPEAN JOURNAL OF MEDICINAL CHEMISTRY
http://www.elsevier.com/locate/ejmech

Original article

Synthesis, binding properties and receptor docking of 4-halo-6-[2-(4-arylpiperazin-1-yl)ethyl]-1*H*-benzimidazoles, mixed ligands of D_2 and 5-HT_{1A} receptors

Deana Andrić [a], Goran Roglić [a], Vladimir Šukalović [b], Vukić Šoškić [c,*], Sladjana Kostić-Rajačić [b]

[a] *Faculty of Chemistry, University of Belgrade, Studentski trg 16, 11000 Belgrade, Serbia*
[b] *Center for Chemistry, Institute for Chemistry, Technology and Metallurgy, Njegoševa 12, 11000 Belgrade, Serbia*
[c] *ProteoSys AG, Carl Zeiss Strasse 51, 55129 Mainz, Germany*

Received 26 April 2007; received in revised form 14 September 2007; accepted 18 September 2007
Available online 7 October 2007

Abstract

In this publication we are describing synthesis, binding properties, and receptor docking of 4-halo-6-[2-(4-arylpiperazin-1-yl)ethyl]-1*H*-benzimidazoles, a new compounds with potential antipsychotics properties. Affinity towards the dopamine D_1-like and D_2-like, and serotonin 5-HT_{1A} receptors was evaluated using the radioligand binding assays. All compounds tested had affinity for the D_2-like and 5-HT_{1A} receptors, but were inactive towards the D_1-like receptor. Halogenated 6-[2-(4-arylpiperazin-1-yl)ethyl]-1*H*-benzimidazoles showed higher affinity compared to their nonhalogenated congeners. *In silico* docking analysis of selected ligands was performed in order to explain the results of binding assays. Our analysis suggests that stabilizing interactions between the halogen atom at the benzimidazole ring and the Ser-122 of the D_2-like and Trp-358 of the 5-HT_{1A} receptor. Energy contributions for these interactions were calculated using the *ab initio* method.

Keywords: Dopamine receptor; Serotonin receptor; Rational drug design

1. Introduction

The discovery of phenothiazine in 1952 marked the starting point of the era of modern pharmacologic treatment of psychosis. A series of drugs with similar properties—mostly antagonists of dopamine D_2-like receptors, now referred to as ''classical antipsychotics''—were subsequently developed [1]. The classical antipsychotics, however, are associated with severe side effects and are inefficient against negative symptoms of schizophrenia, such as social withdrawal [2–4]. The new hope came with the antipsychotics of second generation, also known as the ''atypical antipsychotics'' or ''dopamine–serotonin system stabilizers'' [5]. These derivatives possess a combined antagonistic effect towards D_2-like receptors and serotonin 5-HT_2 receptors (e.g., clozapine, risperidone, and olanzapine), or act as partial agonists of D_2-like receptors and interacts with 5-HT_{1A} receptors or other CNS targets (aripiprazole and bifeprunox) [2,3].

Another pharmacological approach, which has been gaining ground steadily, involves combining D_2 antagonism and 5-HT_{1A} agonism in the same molecule [6–8]. Therefore, parameters like D_2/5-HT_{1A} affinity ratio as well as 5-HT_{1A} intrinsic activities have been recognized as important *in vitro* indicators for selection of lead candidates [8]. Our previous results have shown that 5-[2-(4-arylpiperazin-1-yl)ethyl]-1*H*-benzimidazoles exert a mixed D_2/5-HT_{1A} affinity [9] and therefore can be considered as candidates for this new class of antipsychotics. We have also observed that halogenation of benzimidazole

* Corresponding author. Tel.: +49 6131 50 192 47; fax: +49 6131 50 192 12.
E-mail address: vukic.soskic@proteosys.com (V. Šoškić).

0223-5234/$ - see front matter © 2007 Elsevier Masson SAS. All rights reserved.
doi:10.1016/j.ejmech.2007.09.027

moiety has a pronounced effect on the D_2-like [10] and 5-HT_{1A} (data not yet published) receptor affinity.

The effect of halogen on the stability of receptor–ligand complex can be explained by a charge transfer or hydrogen bonding of the halogens (so-called "halogen bonding") and the receptor molecules [11–13]. The aim of the present study was to develop a molecular model that would explain the affinity of 4-halo-6-[2-(4-arylpiperazin-1-yl)ethyl]-1*H*-benzimidazoles towards the D_2-like and 5-HT_{1A} receptors. Therefore, newly synthesized 4-halo-6-[2-(4-arylpiperazin-1-yl)ethyl]-1*H*-benzimidazoles were evaluated for their ability to bind D_1-like, D_2-like and 5-HT_{1A} receptors, and were further subjected to docking analysis using the binding site models of D_2-like and 5-HT_{1A} receptors and the *ab initio* calculation for putative C–Halogen···N and C–Halogen···HN interactions.

2. Chemistry

Synthetic route and chemical structures of the compounds synthesized in the present study are shown in Scheme 1. Key intermediary compounds, 2-halo-4-(2-chloroethyl)-6-nitroanilines (**4a**,**b**), were obtained as previously described [10]. Alkylation of arylpiperazines using those compounds gave rise to 2-halo-6-nitro-4-[2-(4-arylpiperazin-1-yl)ethyl]anilines **5a**,**b**–**9a**,**b**. Reduction of nitroanilines **5a**,**b**–**9a**,**b** by Ra-Ni/hydrazine provided 2-amino-3-halo-5-[2-(4-arylpiperazin-1-yl)-ethyl]phenylamines **10a**,**b**–**14a**,**b**. Finally, a reaction of diamines **10a**,**b**–**14a**,**b** with formic acid yielded 4-halo-6-[2-(4-arylpiperazin-1-yl)ethyl]-1*H*-benzimidazoles **15a**,**b**–**19a**,**b**.

3. Pharmacology

The affinities (K_i values, Table 1) of the newly synthesized 4-halo-6-[2-(4-arylpiperazin-1-yl)ethyl]-1*H*-benzimidazoles (**15a**,**b**–**19a**,**b**) as well as for nonhalogenated analogues 5-[2-(4-arylpiperazin-1-yl)ethyl]-1*H*-benzimidazoles (**20**–**24**) [9] towards D_1-like, D_2-like and 5-HT_{1A} receptors were evaluated using *in vitro* binding assays.

4. Molecular modeling and *ab initio* calculations

All ligands were docked into the binding-pocket model of the D_2-like receptor defined by Teeter et al. [14], according to the procedure previously described [15]. Docking to the 5-HT_{1A} receptor was performed as previously described [16]. *Ab initio* MP2 calculations of relative stabilizing energy contribution of the C–Halogen···HN and C–Halogen···HO were performed using Gaussian 03W suit. In these calculations MP2/6-31+G* basic set was used, including counterpoise correction to BSSE. Calculations were performed on the couples: ligand–Ser-122 (D_2-like receptor, Table 2) and ligand–Trp-358 (5-HT_{1A} receptor, Table 2) that were incised from docked ligand–receptor complexes, taking care that the original geometry is preserved.

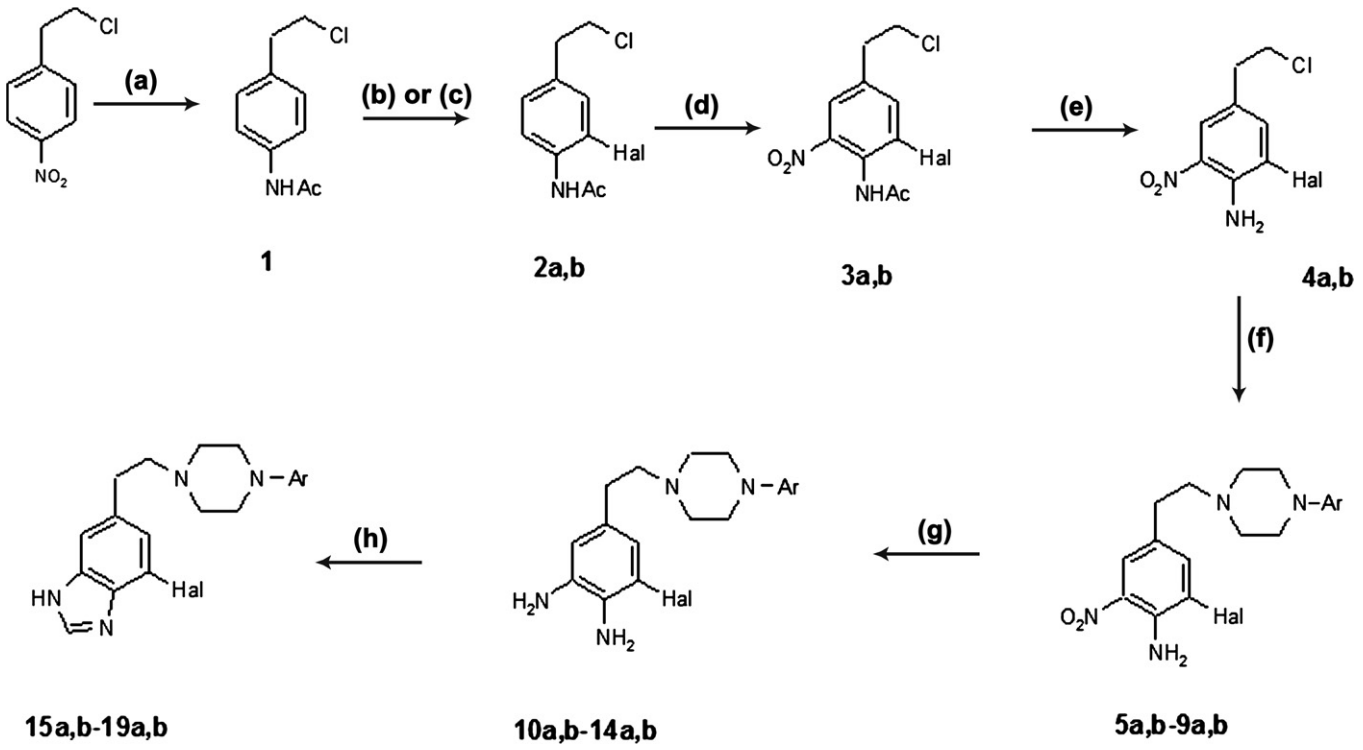

Scheme 1. Synthetic pathways for 4-halo-6-[2-(4-arylpiperazin-1-yl)ethyl]-1*H*-benzimidazoles; (a) $SnCl_2$, EtOH, Ac_2O; (b) SO_2Cl_2, $CHCl_3$; (c) Br_2, AcOH; (d) Ac_2O, HNO_3/H_2SO_4; (e) 4 N HCl; (f) DMF, KI, K_2CO_3, arylpiperazine; (g) Ra-Ni, hydrazine; (h) HCO_2H. Hal is Cl for all compounds labeled with **No.a** and Br for the one labeled with **No.b**.

Table 1
Structure and binding properties of the ligands described in this study

No	Ar	K_i (nM)		
		D_1	D_2	5-HT_{1A}
	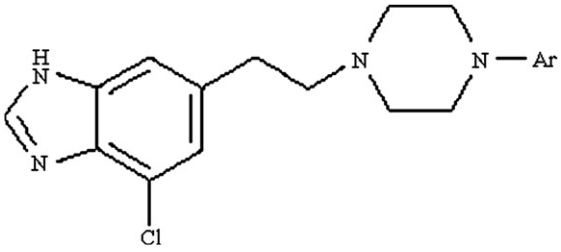			
15a	Phe	>1000	84.7 ± 11	89.6 ± 18
16a	2-MeOPhe	>1000	5.49 ± 0.8	5.2 ± 0.4
17a	2-ClPhe	>1000	19.1 ± 2.4	45.6 ± 3.2
18a	3-CF_3Phe	>1000	200 ± 19	20.7 ± 2.1
19a	Pyrimidin-2-yl	>1000	550 ± 25	529.6 ± 29
	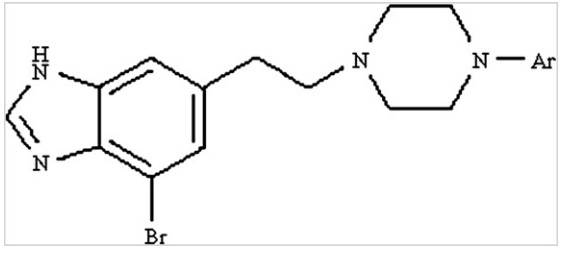			
15b	Phe	>1000	61.9 ± 3.3	24.1 ± 3.3
16b	2-MeOPhe	>1000	0.56 ± 0.09	1.4 ± 0.2
17b	2-ClPhe	>1000	5.77 ± 1.2	0.14 ± 0.06
18b	3-CF_3Phe	>1000	14.6 ± 3.2	10.3 ± 0.5
19b	Pyrimidin-2-yl	>1000	26.7 ± 22	129 ± 15
	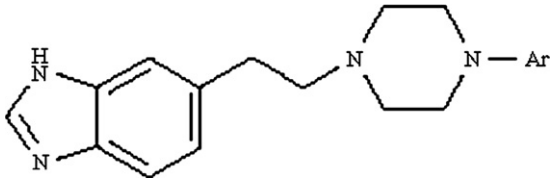			
20	Phe	>1000	138 ± 23	197 ± 52
21	2-MeOPhe	nd	13.1 ± 1.0	20.3 ± 3.0
22	2-ClPhe	nd	59.7 ± 3.2	243 ± 54
23	3-CF_3Phe	>1000	273 ± 38	33.0 ± 4.0
24	Pyrimidin-2-yl	nd	>1000	>1000

Values are the means ± S.E.M. of 3–4 independent experiments done in triplicate, performed at five ([^{3}H]SCH 2339) and eight competing ligand concentrations ([^{3}H]spiperone and [^{3}H]8-OH-DPAT).

5. Results and discussion

5.1. Pharmacology

Herein tested compounds were poor competitors of specific radioligands for the D_1-like receptor, while showing affinity towards D_2-like and 5-HT_{1A} receptor. Halogenation increased the affinity of new ligands towards both types of receptors in the following order: Br > Cl > H. Besides, *N*-trifluoromethylpiperazine **18a** and 4-bromoimidazoles (**15b**, **17b** and **19b**) showed some 5-HT_{1A} receptor selectivity ($p < 0.05$; Table 1). The most potent 5-HT_{1A} receptor ligand was 4-bromo-6-{2-[4-(2-chlorophenyl)piperazin-1-yl]ethyl}-1*H*-benzimidazole (**17b**), where halogenation increased the affinity towards the D_2-like and 5-HT_{1A} receptor by 12.0 and 1735 times, respectively. The most potent ligand for the D_2-like receptor was 4-bromo-6-{2-[4-(2-methoxyphenyl)piperazin-1-yl]ethyl}-1*H*-benzimidazole (**16b**), where halogenation increased the affinity towards the D_2-like and 5-HT_{1A} receptor by 40.0 and 12.9 times, respectively.

Table 2
Relative stabilizing energy calculation for 4-halo-benzimidazole–Ser-141 (D_2-like receptor) and 4-halo-benzimidazole–Trp-358 (5-HT_{1A} receptor) interactions

	Ligand–D_2 -like receptor interaction	Ligand–5-HT_{1A} receptor interaction
Molecular model	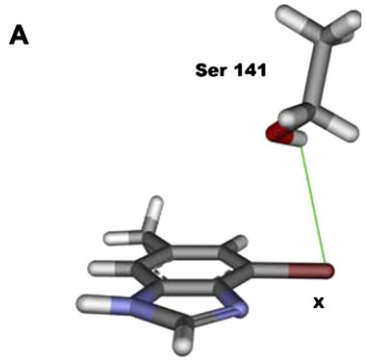	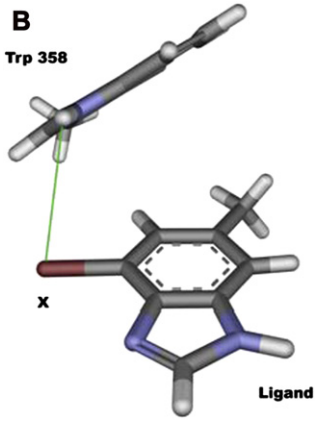
Calculated stabilizing energy (kcal mol^{-1})	X = H; $E = 0.0$ X = Cl; $E = -0.99$ X = Br; $E = -1.13$	X = H; $E = 0.0$ X = Cl; $E = -0.46$ X = Br; $E = -0.63$

A: Sketch of the benzimidazole part of ligands (X: H, Cl or Br) and Ser-122 (D_2-like receptor), **B**: sketch of the benzimidazole part of ligand (X: H, Cl or Br) and Trp-358 (5-HT_{1A} receptor) that were incised from docked ligand–receptor complexes.

This increase in affinity suggests an attractive interaction between the halogen atom and some molecular moiety in the binding pocket of both D_2-like and 5-HT_{1A} receptors. Charge transfer and halogen bonding interactions have been already described as important in some chemical and biological systems [11–13]. To test the involvement of those interactions in our system, we performed *in silico* docking of halogenated ligands to the models of D_2-like and 5-HT_{1A} receptors.

5.2. Docking to the D_2-like receptor

Docking of 4-halo-6-{2-[4-arylpiperazin-1-yl]ethyl}-1*H*-benzimidazoles (**15a**,**b**–**19a**,**b**) and their nonhalogenated congeners (**20**–**24**) to the to the D_2-like receptor binding site revealed that (i) close interaction of the protonated N1 of the piperazine ring with Asp-86, (ii) hydrogen bonds between the benzimidazole nitrogens and Ser-141 and Ser-122, and (iii) edge-to-face interactions of the aromatic ring or the arylpiperazine part of and the rings of Phe-178, Tyr-216 and Trp-182 represent main stabilizing forces. Distances between receptor–ligand atom pairs are shown in Fig. 1.

In our previous publication [15] we reported an interaction of benzimidazole catechol bioisostere with both Ser-122 and Ser-144 of the D_2-like receptor. Docking of halogenated compounds indicates close interaction only of Ser-122, which can be explained by halogen-directed reorientation of the benzimidazole part of the ligand towards the formation of hydrogen bond with Ser-122 (distance Ser-122(OH)/N^{bzi}, 2.63 Å (**16a**) and Ser-122(OH)/N^{bzi}, 2.67 Å (**16b**); Fig. 1) and with the charge transfer interaction [11,12] of Ser-122 and the halogen (distance Ser-122(OH)/Cl, 2.95 Å (**16a**) and Ser-122(OH)/Br, 2.87 Å (**16b**); Fig. 1).

5.3. Docking to the 5-HT_{1A} receptor

Docking of 4-halo-6-{2-[4-arylpiperazin-1-yl]ethyl}-1*H*-benzimidazoles (**15a**,**b**–**19a**,**b**) and their nonhalogenated congeners (**20**–**24**) to the 5-HT_{1A} receptor binding site revealed: (i) a salt bridge between the protonated N1 of the piperazine ring and negatively charged Asp-116, (ii) hydrogen bonds between the substituents on the benzimidazole part and Ser-199 and Trp-358, and (iii) edge-to-face interactions of the aromatic ring or arylpiperazine part with Phe-361 and Tyr-390. Distances between the receptor–ligand atom pairs are shown in Fig. 2. Docking analysis showed that this increase in affinity is likely due to a charge transfer interaction between the halogen atoms of the ligands and partially positive charges of hydrogen atoms linked to the nitrogen of Trp-358 (Fig. 2). The distances between C–Cl (ligand **16a**) and C–Br (ligand **16b**) and HN of Trp-358 (ligand **16a**) are 3.61 Å and 3.53 Å, respectively, with the angle of about 90° falling well in the range of this type of interactions [11–13]. The small angle measured between C–Halogen···Trp-358 eliminates the possibility of halogen binding, which is considered to be a near-linear interaction (nucleophile–C–halogen angle of 160°–180°) [13].

Therefore, a disproportionally high affinity of ligand **17b** is difficult to explain solely on the basis of the formation of one new charge transfer interaction. Addressing this issue in fine detail will be possible with the publication of a high-resolution model of the receptor–ligand complex.

5.4. Ab initio calculations of C–Halogen···N and C–Halogen···H–N interactions

In support our hypothesis that charge transfer interactions play a significant stabilizing role in the formation of

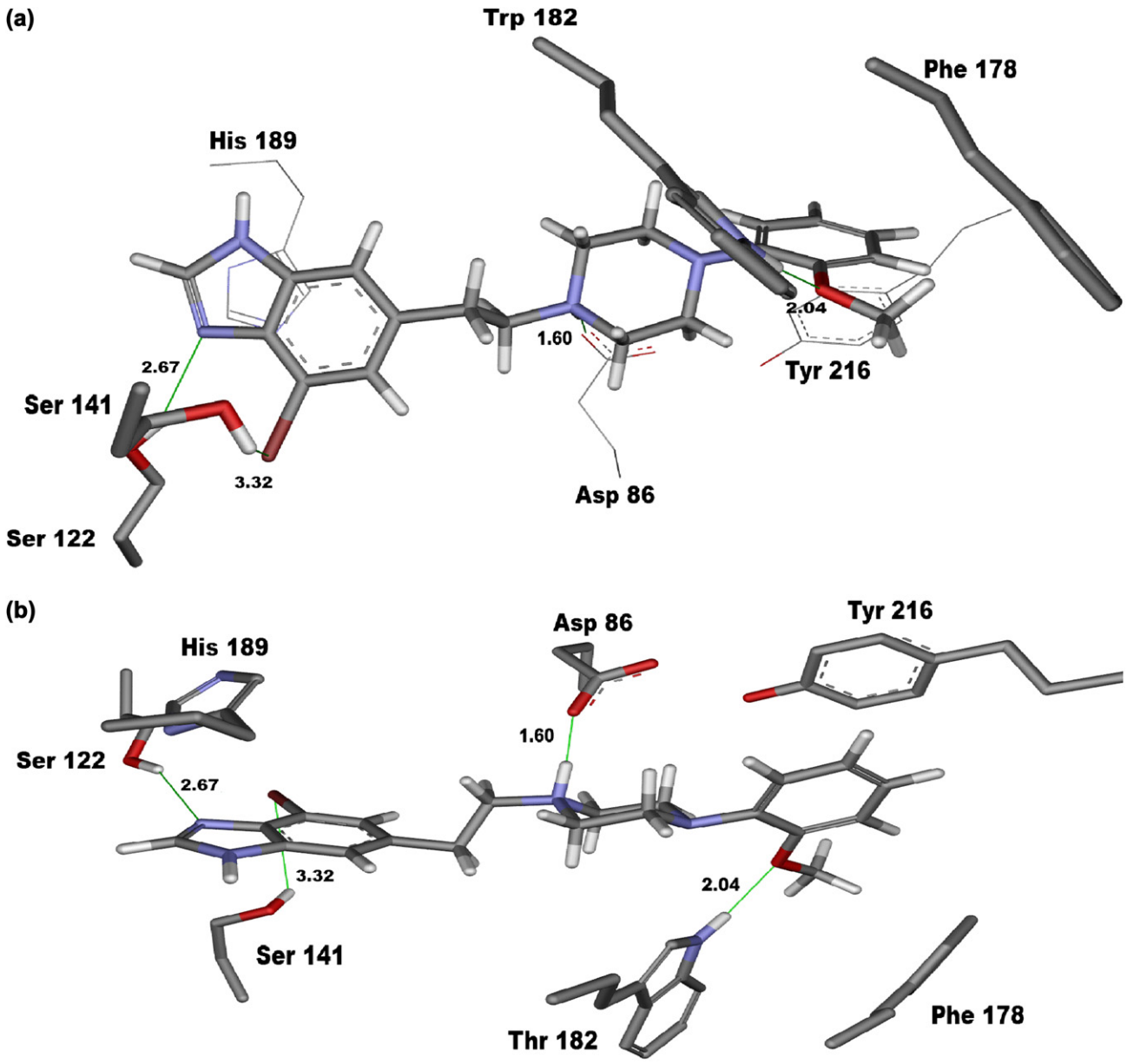

Fig. 1. View of the interaction between D_2-like receptor binding site and **16b**. Docking of ligand **16b** to D_2-like receptor is presented. Images are showing only key amino acid residues of the receptor binding pocket. Figures a and b shows docking of **16b** viewed from different angles.

complexes between our ligands and D_2-like and 5-HT_{1A} receptors, *ab initio* MP2 calculations were performed. Relative stabilizing energy contribution of the C—halogen···HN(Trp-358) and C—halogen···HO(Ser-122) interactions are presented in Table 2. The calculations show that there is a gain in energy of the system, due to the charge transfer interaction between halogen atoms of the ligand and the counterpart polar group of the receptor, wherein Br has higher effect than Cl.

6. Conclusion

4-Halo-6-[2-(4-arylpiperazin-1-yl)ethyl]-1*H*-benzimidazoles have higher affinity towards both D_2-like and 5-HT_{1A} receptors, than their nonhalogenated analogues. Docking analysis using the at D_2-like receptor model revealed that introduction of halogen atom in the benzimidazole part of the ligand promotes formation of a hydrogen bond and charge transfer interaction of between the halogen and the Ser-122. Similarly, charge transfer interaction was observed between halogenated ligands and the Trp-358 residue of 5-HT1A receptor. Results of the docking analysis were supported by *ab initio* calculations of putative charge transfer interactions. Bromo derivatives showed a higher affinity than their chloro-counterparts, but no satisfactory explanation could be found at this point. Based on the high affinity and favorable D_2/5-HT_{1A} affinity ratio, compound **17b** is a good candidate for further pharmacological studies.

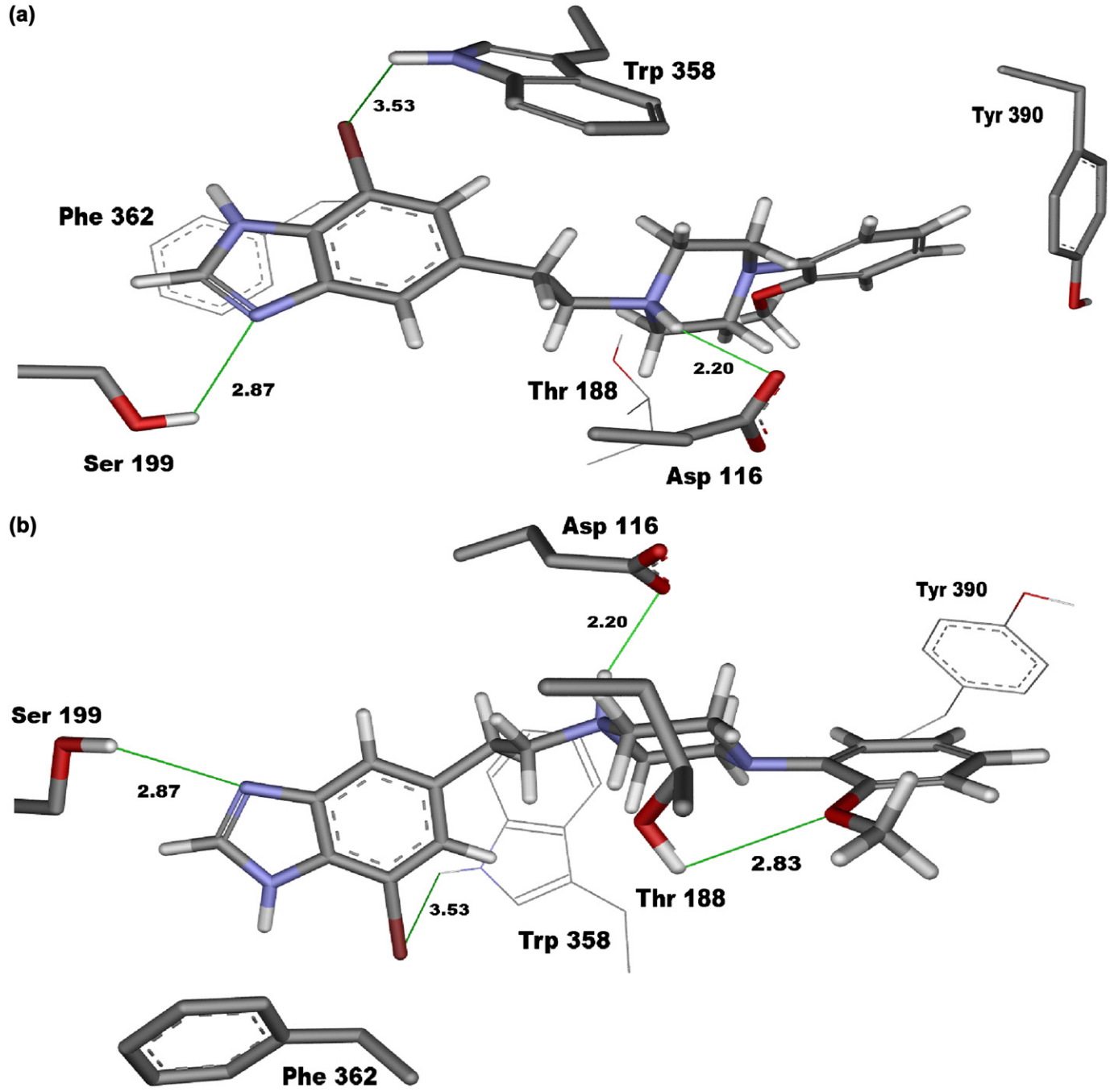

Fig. 2. View of the interaction between 5-HT_{1A} receptor binding site and ligand **16b.** Docking of ligand **16b** to 5-HT_{1A} receptor is presented. Images are showing only key amino acid residues of the receptor binding pocket. Figures a and b shows docking of **16b** viewed from different angles.

7. Experimental protocols

7.1. General

A Boetius PHMK apparatus (VEB Analytic, Dresden, Germany) was used to determine melting points, presented here as uncorrected. ^{1}H NMR (at 200 MHz) and ^{13}C NMR (at 50 MHz) spectra were recorded on a Gemini 2000 spectrometer (Varian, Palo Alto, CA, USA) with $CDCl_3$ as a solvent, unless otherwise stated, are reported in parts per million using tetramethylsilane as the internal standard. The IR spectra were run on a Perkin Elmer 457 Grating FT Infrared Spectrophotometer (Perkin Elmer, Beaconsfield, UK). The mass spectra were determined by field desorption mass spectroscopy on Finnigan Mat 8230 mass spectrometer (Finnigan, Bremen, Germany). For analytical thin-layer chromatography Merck (Darmstadt, Germany) F-256 plastic-backed thin-layer silica gel plates were used. Chromatographic purifications were performed on Merck-60 silica gel columns, 230–400 mesh ASTM, under medium pressure (dry column flash chromatography). All reagents and solvents used in this work were obtained from Aldrich and were used without further purification. Solutions

were routinely dried over anhydrous Na_2SO_4 *prior* to evaporation.

7.2. Molecular modeling

7.2.1. D_2-like receptor binding site

All ligands were docked into the binding pocket of the D_2-like receptor, according to the procedure we described earlier [15]. Shortly, the model of the D_2 DAR transmembrane helices was constructed directly from the bacteriorhodopsin coordinates derived from two-dimensional electron diffraction experiments, but the orientations of all TM domains were subsequently adjusted in order to mimic the topology of the TM domains of rhodopsin [14,17]. This model was tested for its ability to accommodate rigid agonist and semi-rigid antagonist molecules which were docked into the putative binding pocket with stabilizing interactions. The model is consistent with structure–activity relationships of agonists and antagonists that interact with the receptor [14] and with site-directed mutagenesis data [18–20].

7.2.2. 5-HT_{1A} receptor binding site

The model of the human 5-HT_{1A} was built as described previously [16] using crystal structures of bovine rhodopsin (PDB codes 1F88, 1HZX, and 1L9H) was a template. Comparative modeling by means of the MODELER program [21], which is part of the Insight II package from Accelrys, has been used. Our model includes seven transmembrane helices end second extracellular loop e2-loop that can be in direct contact with the ligand [22]. The binding site of the ligand in the 5-HT_{1A} receptor was determined starting from the fact that for the ligand activity formation of the salt bridge between protonated piperazine nitrogen and Asp-116 (Asp 3.32) is necessary [23], active site search procedure from binding site analysis module (Insight II) [24] was used to select all amino acid residues forming the cavity near Asp-116. The binding site defined in the previous step was further refined by manually excluding all amino acid residues that cannot come in direct contact with the inside of the cavity.

7.2.3. Docking

All ligands used in docking analysis were modeled using Accelrys Insight II program build module. Initial geometry was optimized until energy minima were reached using inbuilt geometry optimization routine. Geometry obtained in this manner was starting point for docking analysis.

Docking of the selected ligands presented in Table 1 was done by simulated annealing using the Affinity module from Insight on SGI Octane2 workstation [24]. All ligands were docked as a protonated, using the CFF91 force field. Amino acid residues charges were adjusted where needed. Protein binding site was determined by combining results from experimental data and Insight II bind site analysis module. Initial position of the ligand in the bind site, was arbitrary, while protonated nitrogen on ligand part was kept in close proximity of Asp-86 of D_2-like or Asp-116 of 5-HT_{1A} receptor. After initial ligand placement no further constrains were applied and docking procedure based on Monte Carlo methodology was carried out. Up to 100 structures were produced in every run and each finally optimized in order remove steric interaction with gradient limit of 0.0042 kJ mol^{-1} or 4000 optimization steps.

Obtained docked structures were examined, and those with lowest total energy were further filtered to obtain docking structures with best ligand fit. We selected structures based on following criteria: lowest total energy of the complex, shortest salt bridge formed between Asp-86 of D_2-like or Asp-116 of 5-HT_{1A} receptor and proton on nitrogen, chair conformation of arylpiperazine ring and aryl part of the molecule positioned in rear hydrophobic pocket of the ligand. After an initial criterion was satisfied, second step was examination of different interactions that can be formed between receptor and ligand (hydrogen bonds, aromatic–aromatic interactions, etc.). In that way, the best possible docking structures were selected. Structures were rendered using povray raytracer v3.6 [25].

7.3. Ab initio calculations

Gaussian 03 suite [26] was used to carry on calculation of energy contribution of the chosen Ligand–Halogen···AA dimer. Mutual orientation interacting groups were taken from docking analysis results. The stabilization energies of the paired structures were calculated as a difference between dimmer and separate molecular entities using a MP2HF method and 6-31+G* basis set. To compensate for basis set superposition error, counterpoise method suggested by Boys and Bernardi [27] was used.

7.4. Chemistry

7.4.1. General procedure for the synthesis of 2-halo-6-nitro-4-[2-(4-arylpiperazin-1-yl)ethyl]anilines **5a,b–9a,b**

To 10.0 mmol solution of arylpiperazine in 50.0 ml DMF, 12.0 mmol of 2-halo-4-(2-chloroethyl)-6-nitroaniline (**4a**,**b**), 6.0 g K_2CO_3 and 0.1 g of KI were added. The mixture was stirred at 80 °C for 12 h. After cooling, the precipitate was removed and the filtrate was evaporated *in vacuo*. The residue was dissolved in CH_2Cl_2 and obtained products purified by MPLC using CH_2Cl_2 as the eluent.

*7.4.1.1. 2-Chloro-6-nitro-4-[2-(4-phenylpiperazin-1-yl)ethyl]-aniline (**5a**).* Yield: 69%; m.p. 104 °C; ^{1}H NMR: δ 2.57–2.80 (m, 8H), 3.20–3.25 (m, 4H), 6.45 (s, 2H, NH_2), 6.87–6.97 (m, 3H, ArH), 7.22–7.32 (m, 2H, ArH), 7.45 (d, 1H, $J = 2.2$ Hz, ArH), 7.97 (d, 1H, $J = 2$ Hz, ArH).

*7.4.1.2. 2-Bromo-6-nitro-4-[2-(4-phenylpiperazin-1-yl)ethyl]-aniline (**5b**).* Yield: 72%; m.p. 110 °C; ^{1}H NMR: δ 2.57–2.80 (m, 8H), 3.20–3.25 (m, 4H), 6.51 (s, 2H, NH_2), 6.83–6.96 (m, 3H, ArH), 7.24–7.32 (m, 2H, ArH), 7.62 (d, 1H, $J = 2$ Hz, ArH), 8.01 (d, 1H, $J = 2$ Hz, ArH).

*7.4.1.3. 2-Chloro-6-nitro-4-{2-[4-(2-methoxyphenyl)piperazin-1-yl]ethyl}aniline (**6a**).* Yield: 76%; m.p. 97 °C; ^{1}H NMR: δ 2.59–2.81 (m, 8H), 3.10–3.21 (m, 4H), 3.87 (s, 3H, OCH_3),

6.45 (s, 2H, NH_2), 6.85–7.02 (m, 4H, ArH), 7.45 (d, 1H, $J = 2$ Hz, ArH), 7.97 (d, 1H, $J = 2$ Hz, ArH).

*7.4.1.4. 2-Bromo-6-nitro-4-{2-[4-(2-methoxyphenyl)piperazin-1-yl]ethyl}aniline (**6b**).* Yield: 67%; m.p. 95 °C; ^{1}H NMR: δ 2.58–2.79 (m, 8H), 3.12 (s, 4H), 3.87 (s, 3H, OCH_3), 6.51 (s, 2H, NH_2), 6.85–7.02 (m, 4H, ArH), 7.61 (d, 1H, $J = 2$ Hz, ArH), 8.00 (d, 1H, $J = 2$ Hz, ArH).

*7.4.1.5. 2-Chloro-6-nitro-4-{2-[4-(2-chlorophenyl)piperazin-1-yl]ethyl}aniline (**7a**).* Yield: 79%; m.p. 98 °C; ^{1}H NMR: δ 2.60–2.81 (m, 8H), 3.09–3.13 (m, 4H), 6.46 (s, 2H, NH_2), 6.93–7.09 (m, 2H, ArH), 7.19–7.27 (m, 1H, ArH), 7.36 (dd, 1H, $J = 4$ Hz, $J = 2$ Hz, ArH), 7.46 (d, 1H, $J = 2$ Hz, ArH), 7.98 (d, 1H, $J = 2$ Hz, ArH).

*7.4.1.6. 2-Bromo-6-nitro-4-{2-[4-(2-chlorophenyl)piperazin-1-yl]ethyl}aniline (**7b**).* Yield: 76%; m.p. 128 °C; ^{1}H NMR: δ 2.60–2.80 (m, 8H), 3.08–3.13 (m, 4H), 6.52 (s, 2H, NH_2), 6.94–7.09 (m, 2H, ArH), 7.19–7.23 (m, 1H, ArH), 7.36 (dd, 1H, $J = 6.2$ Hz, $J = 1.8$ Hz, ArH), 7.62 (d, 1H, $J = 2$ Hz, ArH), 8.02 (d, 1H, $J = 2$ Hz, ArH).

*7.4.1.7. 2-Chloro-6-nitro-4-(2-{4-[3-(trifluoromethyl)phenyl]-piperazin-1-yl}ethyl)aniline (**8a**).* Yield: 59%; oil; ^{1}H NMR: δ 2.58–2.78 (m, 8H), 3.23–3.28 (m, 4H), 6.44 (s, 2H, NH_2), 7.08–7.21 (m, 3H, ArH), 7.42 (t, 1H, $J = 8$ Hz, ArH), 7.59 (d, 1H, $J = 2$ Hz, ArH), 7.97 (d, 1H, $J = 2$ Hz, ArH).

*7.4.1.8. 2-Bromo-6-nitro-4-(2-{4-[3-(trifluoromethyl)phenyl]-piperazin-1-yl}ethyl)aniline (**8b**).* Yield: 64%; oil; ^{1}H NMR: δ 2.58–2.71 (m, 8H), 3.24–3.29 (m, 4H), 6.52 (s, 2H, NH_2), 7.05–7.39 (m, 4H, ArH), 7.62 (d, 1H, $J = 2$ Hz, ArH), 8.04 (d, 1H, $J = 2$ Hz, ArH).

*7.4.1.9. 2-Chloro-6-nitro-4-{2-[4-(2-pyrimidinyl)piperazin-1-yl]ethyl}aniline (**9a**).* Yield: 69%; m.p. 115 °C; ^{1}H NMR: δ 2.54–2.65 (m, 6H), 2.72–2.80 (m, 2H), 3.83–3.88 (m, 4H), 6.45–6.52 (m, 3H, NH_2, ArH), 7.45 (d, 1H, $J = 2$ Hz, ArH), 7.97 (d, 1H, $J = 2$ Hz, ArH), 8.28 (d, 2H, $J = 4.6$ Hz, ArH).

*7.4.1.10. 2-Bromo-6-nitro-4-{2-[4-(2-pyrimidinyl)piperazin-1-yl]ethyl}aniline (**9b**).* Yield: 63%; m.p. 118 °C; ^{1}H NMR: δ 2.54–2.65 (m, 6H), 2.71–2.80 (m, 2H), 3.82–3.88 (m, 4H), 6.47–6.52 (m, 3H, NH_2, ArH), 7.62 (d, 1H, $J = 2$ Hz, ArH), 8.01 (d, 1H, $J = 2$ Hz, ArH), 8.31 (d, 2H, $J = 4.6$ Hz, ArH).

*7.4.2. General procedure for synthesis of 2-amino-3-halo-5-[2-(4-arylpiperazin-1-yl)ethyl]phenylamines **10a**,**b**–**14a**,**b***

Raney-Ni (0.06–0.08 g) was added in small portions to a stirring solution of 2 mmol of nitro compound (**5a**,**b**–**9a**,**b**) in 5 ml EtOH, 10 ml 1,2-dichloro-ethane and 0.9 ml hydrazine hydrate at 30 °C. After the addition of Ra-Ni was completed, the mixture was heated in a water bath (50 °C, 60 min) and filtered through celite. The filtrate was evaporated *in vacuo* and crude products were used for further syntheses.

*7.4.3. Synthesis of 4-chloro-6-[2-(4-arylpiperazin-1-yl)-ethyl]-1H-benzimidazoles (**15a**–**19a**) and 4-bromo-6-[2-(4-arylpiperazin-1-yl)ethyl]-1H-benzimidazoles (**15b**–**19b**)*

Diamine of 2 mmol (**10a**,**b**–**14a**,**b**) and 0.44 ml (7.3 mmol) of 98% formic acid were heated in an oil bath at 100 °C for 2 h. After cooling to ambient temperature, 15 ml of 10% $NaHCO_3$ was added and the product extracted with CH_2Cl_2. The solvent was removed *in vacuo* and the residue chromatographed on silica gel.

*7.4.3.1. 4-Chloro-6-[2-(4-phenylpiperazin-1-yl)ethyl]-1H-benzimidazole (**15a**).* Yield: 80%; m.p. 186 °C; IR (cm^{-1}): 634, 693, 1139, 1239, 1410, 1494, 1593, 2826; ^{1}H NMR (DMSO-d_6): δ 2.55–2.65 (m, 6H), 2.89 (t, 2H, $J = 8.2$ Hz), 3.13 (s, 4H), 6.77 (t, 1H, $J = 7.2$ Hz, ArH), 6.93 (d, 2H, $J = 7.6$ Hz, ArH), 7.17–7.25 (m, 3H, ArH), 7.38 (s, 1H, ArH), 8.25 (s, 1H, CH), 12.67 (s, 1H, NH); ^{13}C NMR (DMSO-d_6): δ 32.60 (CH_2), 48.29 ($2CH_2$), 52.81 ($2CH_2$), 60.07 (CH_2), 110.82 (CH), 113.24 (C–Cl), 115.53 (2CH), 118.99 (CH), 122.58 (CH), 128.60 (C), 129.14 (2CH), 133.85 (C), 135.98 (C), 142.87 (CH), 151.29 (C–N); MS: *m/e* (100) 340.1 (M^+).

*7.4.3.2. 4-Bromo-6-[2-(4-phenylpiperazin-1-yl)ethyl]-1H-benzimidazole (**15b**).* Yield: 85%; m.p. 188 °C; IR (cm^{-1}): 762, 1235, 1499, 1599, 2815, 3384; ^{1}H NMR: δ 2.63–2.74 (m, 6H), 2.92–2.99 (m, 2H), 3.13–3.27 (m, 4H), 6.83–6.96 (m, 3H, ArH), 7.13–7.45 (m, 4H, ArH), 8.07 (s, 1H, CH); ^{13}C NMR (DMSO-d_6): δ 32.56 (CH_2), 48.35 ($2CH_2$), 52.85 ($2CH_2$), 60.17 (CH_2), 110.86 (C–Br), 111.35 (CH), 115.50 (2CH), 118.94 (CH), 125.46 (CH), 128.63 (C), 129.13 (2CH), 133.49 (C), 136.69 (C), 142.67 (CH), 151.26 (C–N); MS: *m/e* (100) 385.9 (M^+).

*7.4.3.3. 4-Chloro-6-{2-[4-(2-methoxyphenyl)piperazin-1-yl]-ethyl}-1H-benzimidazole (**16a**).* Yield: 78%; m.p. 84 °C; IR (cm^{-1}): 750, 1027, 1241, 1500, 2814; ^{1}H NMR: δ 2.77–2.85 (m, 6H), 2.98–3.10 (m, 2H), 3.21 (s, 4H), 3.91 (s, 3H, OCH_3), 6.89–7.11 (m, 4H, ArH), 7.18 (s, 1H, ArH), 7.30 (s, 1H, ArH), 8.10 (s, 1H, CH); ^{13}C NMR: δ 32.10 (CH_2), 50.29 (CH_3), 53.31 ($2CH_2$), 55.33 ($2CH_2$), 60.52 (CH_2), 111.19 (CH), 112.12 (CH), 113.22 (C–Cl), 118.29 (CH), 121.04 (CH), 123.23 (CH), 123.48 (CH), 128.62 (C), 133.96 (C), 135.92 (C), 140.23 (C–O), 141.25 (CH), 152.23 (C–N); MS: *m/e* (100) 370.1 (M^+).

*7.4.3.4. 4-Bromo-6-{2-[4-(2-methoxyphenyl)piperazin-1-yl]-ethyl}-1H-benzimidazole (**16b**).* Yield: 97%; m.p. 49 °C; IR (cm^{-1}): 754, 1244, 1455, 1500, 1593, 3392; ^{1}H NMR (DMSO-d_6): δ 2.86 (s, 6H), 2.95–32.99 (m, 2H), 3.07 (s, 4H), 3.78 (s, 3H, OCH_3), 6.87–7.00 (m, 4H, ArH), 7.36 (s, 1H, ArH), 7.47 (s, 1H, ArH), 8.27 (s, 1H, CH); ^{13}C NMR (DMSO-d_6): δ 30.43 (CH_2), 47.98 (CH_3), 50.35 (CH_2), 52.24 (CH_2), 55.24 (CH_2), 57.79 (CH_2), 60.03 (CH_2), 110.03

(C–Br), 111.18 (CH), 113.14 (CH), 118.33 (CH), 120.93 (CH), 123.90 (CH), 125.67 (CH), 128.27 (C), 132.86 (C), 136.16 (C), 139.21 (C–O), 142.35 (CH), 151.91 (C–N); MS: *m/e* (100) 413.9 (M−2), (90.78) 415.9 (M^+).

*7.4.3.5. 4-Chloro-6-{2-[4-(2-chlorophenyl)piperazin-1-yl]ethyl}-1H-benzimidazole (**17a**).* Yield: 71%; m.p. 122 °C; IR (cm^{-1}): 692, 1039, 1283, 1446, 1479, 2816, 2931; ^{1}H NMR: δ 2.70–2.77 (m, 6H), 2.91–2.99 (m, 2H), 3.09–3.13 (m, 4H), 6.92–7.05 (m, 2H, ArH), 7.17–7.27 (m, 2H, ArH), 7.33–7.38 (m, 2H, ArH), 8.10 (s, 1H, CH); ^{13}C NMR: δ 33.30 (CH_2), 50.98 ($2CH_2$), 53.26 ($2CH_2$), 60.56 (CH_2), 110.62 (CH), 113.22 (C–Cl), 120.30 (CH), 123.36 (CH), 123.74 (C), 127.58 (2CH), 128.67 (C), 130.60 (CH), 130.95 (C), 136.14 (C), 141.58 (CH), 149.02 (C–N); MS: *m/e* (100) 374.0 (M^+).

*7.4.3.6. 4-Bromo-6-{2-[4-(2-chlorophenyl)piperazin-1-yl]ethyl}-1H-benzimidazole (**17b**).* Yield: 93%, m.p. 92 °C; IR (cm^{-1}): 626, 758, 1231, 1283, 1447, 1480, 1581, 2948, 3100, 3410; ^{1}H NMR (DMSO-d_6): δ 2.81 (s, 6H), 2.92–2.99 (m, 2H), 3.06 (m, 4H), 7.01–7.44 (m, 6H, ArH), 8.26 (s, 1H, CH), 12.77 (s, 1H, NH); ^{13}C NMR (DMSO-d_6): δ 31.76 (CH_2), 50.28 ($2CH_2$), 52.58 ($2CH_2$), 59.33 (CH_2), 110.12 (C–Br), 111.22 (CH), 121.05 (CH), 124.23 (C), 125.47 (CH), 127.92 (CH), 128.30 (CH), 130.35 (C), 130.56 (CH), 134.03 (C), 137.04 (C), 141.52 (CH), 149.28 (C–N); MS: *m/e* (100) 419.7 (M^+).

*7.4.3.7. 4-Chloro-6-(2-{4-[3-(trifluoromethyl)phenyl]piperazin-1-yl}ethyl)-1H-benzimidazole (**18a**).* Yield: 94%; m.p. 92 °C; IR (cm^{-1}): 694, 949, 1355, 1450, 1583, 1612, 2820; ^{1}H NMR: δ 2.63–2.75 (m, 6H), 2.91–2.98 (m, 2H), 3.24–3.29 (m, 4H), 7.04–7.10 (m, 3H, ArH), 7.20 (s, 1H, ArH), 7.30–7.41 (m, 2H, ArH), 8.12 (s, 1H, CH); ^{13}C NMR: δ 32.53 (CH_2), 47.69 ($2CH_2$), 52.56 ($2CH_2$), 59.93 (CH_2), 110.95 (CH), 111.02 (CH), 113.20 (C–Cl), 114.79 (CH), 118.90 (CH), 121.96 (CH), 122.42 (C), 127.39 (CH), 129.77 (C), 130.14 (C), 130.39 (C), 136.59 (C), 142.78 (CH), 151.42 (C–N); MS: *m/e* (100) 408.0 (M^+).

*7.4.3.8. 4-Bromo-6-(2-{4-[3-(trifluoromethyl)phenyl]piperazin-1-yl}ethyl)-1H-benzimidazole (**18b**).* Yield: 94%; m.p. 74 °C; IR (cm^{-1}): 695, 950, 1290, 1316, 1353, 1450, 1497, 1575, 2886, 2961; ^{1}H NMR (DMSO-d_6): δ 2.53–2.65 (m, 6H), 2.89 (t, 2H, $J = 8.2$ Hz), 3.20–3.25 (m, 4H), 7.05–7.45 (m, 6H, ArH), 8.25 (s, 1H, CH), 12.75 (br s, 1H, NH); ^{13}C NMR (DMSO-d_6): δ 32.58 (CH_2), 47.78 ($2CH_2$), 52.63 ($2CH_2$), 60.13 (CH_2), 110.93 (C–Br), 111.06 (CH), 111.38 (CH), 114.70 (CH), 118.87 (CH), 122.00 (CH), 125.53 (C), 127.41 (CH), 129.79 (C), 130.15 (C), 130.41 (C), 136.37 (C), 142.72 (CH), 151.48 (C–N); MS: *m/e* (100) 453.9 (M^+).

*7.4.3.9. 4-Chloro-6-{2-[4-(2-pyrimidinyl)piperazin-1-yl]ethyl}-1H-benzimidazole (**19a**).* Yield: 82%; m.p. 157 °C; IR (cm^{-1}): 956, 982, 1358, 1395, 1512, 1549, 1587, 2936; ^{1}H NMR: δ 2.58–2.63 (m, 4H), 2.68–2.73 (m, 2H), 2.92–2.99 (m, 2H), 3.87 (t, 4H, $J = 5.4$ Hz), 6.50 (t, 1H, $J = 5$ Hz, ArH), 7.19 (s, 1H, ArH), 7.27 (s, 1H, ArH), 8.07 (s, 1H, CH), 8.33 (d, 2H, $J = 5$ Hz, ArH), 10.31 (br s, 1H, NH); ^{13}C NMR: δ 32.58 (CH_2), 43.52 ($2CH_2$), 52.68 ($2CH_2$), 60.20 (CH_2), 110.31 (CH), 110.75 (CH), 113.20 (C–Cl), 122.40 (CH), 122.71 (C), 125.45 (CH), 134.89 (CH), 136.24 (C), 142.76 (CH), 158.16 (C–N), 161.49 (C–N); MS: *m/e* (100) 342.1 (M^+).

*7.4.3.10. 4-Bromo-6-{2-[4-(2-pyrimidinyl)piperazin-1-yl]ethyl}-1H-benzimidazole (**19b**).* Yield: 74%; m.p. 166 °C; IR (cm^{-1}): 954, 982, 1258, 1357, 1482, 1548, 1587, 2811; ^{1}H NMR (DMSO-d_6): δ 2.53–2.65 (m, 2H), 2.88 (t, 4H, $J = 8.2$ Hz), 3.41–3.51 (m, 2H), 3.71–3.76 (m, 4H), 6.62 (t, 1H, $J = 4.6$ Hz, ArH), 7.33 (s, 1H, ArH), 7.45 (s, 1H, ArH), 8.27 (s, 1H, CH), 8.36 (d, 2H, $J = 4.8$ Hz, ArH), 12.72 (s, 1H, NH); ^{13}C NMR (DMSO-d_6): δ 32.47 (CH_2), 43.51 ($2CH_2$), 52.65 ($2CH_2$), 60.22 (CH_2), 110.27 (C–Br), 110.95 (CH), 111.12 (CH), 123.07 (C), 123.85 (CH), 125.48 (CH), 135.02 (CH), 136.58 (C), 142.67 (CH), 158.12 (C–N), 161.47 (C–N); MS: *m/e* (100) 386.8 (M^+).

7.5. Membrane preparation, binding assays and data analysis

Specific binding affinities (K_i values, Table 1) were determined as described previously [28,29], by measuring the extent of displacement of the specific tritiated ligands [^{3}H]SCH 23390 (spec. act. 82.1 Ci $mmol^{-1}$) for D_1-like, [^{3}H]spiperone (spec. act. 80.5 Ci $mmol^{-1}$) for D_2-like and [^{3}H]8-OH-DPAT (spec. act. 223 Ci $mmol^{-1}$) for 5-HT_{1A} like receptors (all products of Amersham Buchles GmbH, Germany) to the fresh membrane preparations of the bovine caudate nuclei or hippocampi. The competitive radioassays were performed in sample triplicates. Retained radioactivity was measured by introducing dry filters into 5 ml toluene-based scintillation liquid and counting in a 1219 Rackbeta Wallac scintillation counter.

7.5.1. [^{3}H]SCH 23390 receptor binding assay

Each tube contained 1.0 mM EDTA, 4 mM $MgCl_2$, 1.5 mM $CaCl_2$, 5 mM KCl, 120 mM NaCl, 25 mM Tris–HCl, pH 7.4, caudate nuclei synaptosomal membranes (prot. conc 0.7 mg ml^{-1}), 1.0 nM [^{3}H]SCH 23390 and various concentrations (10^{-5}–10^{-8} M) of the tested compounds in a final volume of 0.5 ml. The tubes were incubated (20 min, 37 °C) and the reaction terminated by vacuum filtration through Whatman GF/B filters. The filters were washed three times with 5 ml of ice-cold 25 mM Tris–HCl buffer, pH 7.4, and bound radioactivity measured by liquid scintillation spectrometry. Specific binding to D_1-like receptors was defined as the difference between the binding in the absence and in the presence of cold 1 μM SCH 23390. The K_d value determined for SCH 23390 was 1.1 nM.

7.5.2. [^{3}H]Spiperone receptor binding assay

[^{3}H]Spiperone binding was assayed in 1.0 mM EDTA, 4 mM $MgCl_2$, 1.5 mM $CaCl_2$, 5 mM KCl, 120 mM NaCl, 25 mM Tris–HCl solution, pH 7.4, caudate nuclei synaptosomal

membranes (prot. conc 0.7 mg ml^{-1}), at 37 °C for 20 min in a total volume of incubation mixture of 1.0 ml. Binding of the radioligand to 5-HT_2 receptors was prevented by 50 μM ketanserin. The K_i values of the tested compounds were determined by competition binding at 0.2 nM of the radioligand and 8–10 different concentrations of each compound (10^{-5}–10^{-10} M). Nonspecific binding was measured in the presence of 1.0 μM (+)-butaclamol. The reaction was terminated by rapid filtration through Whatman GF/C filters, which were further washed three times with 5.0 ml of ice-cold incubation buffer, and retained radioactivity was measured by liquid scintillation spectrometry. The K_d value determined for spiperone was 0.9 nM.

7.5.3. 8-OH-[^{3}H]DPAT receptor binding assay

Each tube contained 1.0 mM EDTA, 4 mM $MgCl_2$, 1.5 mM $CaCl_2$, 5 mM KCl, 120 mM NaCl, 25 mM Tris–HCl, pH 7.4, hippocampi synaptosomal membrane (prot. conc 0.7 mg ml^{-1}), 0.6 nM 8-OH-[^{3}H]DPAT and various concentrations (10^{-5}–10^{-11} M) of the tested compounds in a final volume of 0.5 ml. The tubes were incubated (20 min, 37 °C) and the reaction terminated by vacuum filtration through Whatman GF/B filters. The filters were washed three times with 5 ml of ice-cold 25 mM Tris–HCl buffer, pH 7.4, and bound radioactivity measured by liquid scintillation spectrometry. 5-HT_{1A} specific binding was defined as the difference between the binding in the absence and in the presence of 10 μM 5-hydroxytryptamine. The K_d value determined for 8-OH-DPAT was 1.6 nM.

The inhibition curve and statistical (Student's *t*-test) analysis was performed by GraphPad Prism program packet [30].

Acknowledgements

This work was supported by the Ministry of Science, Technology and Development of Serbia, grant # 142009. The authors wish to thank Dr. V. Pejovic for fruitful discussions and his help in preparation of this manuscript.

References

[1] A. Zhang, J.L. Neumeyer, R.J. Baldessarini, Chem. Rev. 107 (2007) 274–302.
[2] M.S. Stahl, J. Clin. Psychiatry 5 (2003) 9–13.
[3] A. Farah, J. Clin. Psychiatry 7 (2005) 268–274.
[4] R.R. Conley, D.L. Kelly, Curr. Drug Targets CNS Neurol. Disord. 1 (2002) 123–128.
[5] C.A. Tamminga, A. Carlsson, Curr. Drug Targets CNS Neurol. Disord. 1 (2002) 141–147.
[6] S.L.A. Bruins, M.S. Kleven, A. Newman-Tancredi, Neuropharmacology 49 (2005) 996–1006.
[7] M.B. Assie, V. Ravailhe, V. Faucillon, A. Newman-Tancredi, J. Pharmacol. Exp. Ther. 315 (2005) 265–272.
[8] S. Cuisiat, N. Bourdiol, V. Lacharme, A. Newman-Tancredi, F. Colpaert, B. Vacher, J. Med. Chem. 50 (2007) 865–876.
[9] V. Šoškić, J. Joksimović, Curr. Med. Chem. 5 (1998) 493–512.
[10] V. Šukalović, D. Andrić, G. Roglić, S. Kostić-Rajačić, V. Šoškić, Arch. Pham. Pharm. Med. Chem. 337 (2004) 376–382.
[11] P. Metrangolo, H. Neukirch, T. Pilati, G. Resnati, Acc. Chem. Res. 38 (2005) 386–395.
[12] P. Auffinger, F.A. Hays, E. Westhof, P.S. Ho, Proc. Natl. Acad. Sci. U.S.A. 101 (2004) 16789–16794.
[13] P. Politzer, P. Lane, M.C. Concha, Y. Ma, J.S. Murray, J. Mol. Model. 13 (2007) 305–311.
[14] M.M. Teeter, M. Froimowitz, J.B. Stec, C.J. DuRand, J. Med. Chem. 37 (1994) 2874–2888.
[15] V. Šukalović, M. Zlatović, D. Andrić, G. Roglić, S. Kostić-Rajačić, V. Šoškić, Arch. Pham. Pharm. Med. Chem. 337 (2004) 502–512.
[16] M.V. Zlatović, V.V. Šukalović, C. Schneider, G.M. Roglić, Bioorg. Med. Chem. 14 (2006) 2994–3001.
[17] H. Lan, C.J. Durand, M.M. Teeter, K.A. Neve, Mol. Pharmacol. 69 (2006) 185–194.
[18] R.E. Wilcox, W.H. Huang, M.Y. Brusniak, D.M. Wilcox, R.S. Pearlman, M.M. Teeter, C.J. DuRand, B.L. Wiens, K.A. Neve, J. Med. Chem. 43 (2000) 3005–3019.
[19] K.A. Neve, M.G. Cumbay, K.R. Thompson, R. Yang, D.C. Buck, V.J. Watts, C.J. DuRand, M.M. Teeter, Mol. Pharmacol. 60 (2001) 373–381.
[20] J.A. Ballesteros, L. Shi, J.A. Javitch, Mol. Pharmacol 60 (2001) 1–19.
[21] A. Sali, T.L. Blundell, J. Mol. Biol. 234 (1993) 779–815.
[22] L. Shi, J.A. Javitch, Proc. Natl. Acad. Sci. U.S.A. 101 (2004) 440–445.
[23] K. Bondensgaard, M. Ankersen, H. Thøgersen, B.S. Hansen, B.S. Wulff, R.P. Bywater, J. Med. Chem. 47 (2004) 888–899.
[24] SGI Octane2 is trademark of Silicon Graphics, Inc, CA, USA (<http://www.sgi.com>).
[25] PovRay, Persistence of Vision Raytrace is trademark of PovRay team, (<http://www.povray.org>).
[26] M.J. Frisch, G.W. Trucks, H.B. Schlegel, G.E. Scuseria, M.A. Robb, J.R. Cheeseman, J.A. Montgomery Jr., T. Vreven, K.N. Kudin, J.C. Burant, J.M. Millam, S.S. Iyengar, J. Tomasi, V. Barone, B. Mennucci, M. Cossi, G. Scalmani, N. Rega, G.A. Petersson, H. Nakatsuji, M. Hada, M. Ehara, K. Toyota, R. Fukuda, J. Hasegawa, M. Ishida, T. Nakajima, Y. Honda, O. Kitao, H. Nakai, M. Klene, X. Li, J.E. Knox, H.P. Hratchian, J.B. Cross, V. Bakken, C. Adamo, J. Jaramillo, R. Gomperts, R.E. Stratmann, O. Yazyev, A.J. Austin, R. Cammi, C. Pomelli, J.W. Ochterski, P.Y. Ayala, K. Morokuma, G.A. Voth, P. Salvador, J.J. Dannenberg, V.G. Zakrzewski, S. Dapprich, A.D. Daniels, M.C. Strain, O. Farkas, D.K. Malick, A.D. Rabuck, K. Raghavachari, J.B. Foresman, J.V. Ortiz, Q. Cui, A.G. Baboul, S. Clifford, J. Cioslowski, B.B. Stefanov, G. Liu, A. Liashenko, P. Piskorz, I. Komaromi, R.L. Martin, D.J. Fox, T. Keith, M.A. Al-Laham, C.Y. Peng, A. Nanayakkara, M. Challacombe, P.M.W. Gill, B. Johnson, W. Chen, M.W. Wong, C. Gonzalez, J.A. Pople, Gaussian 03, Revision C.02, Gaussian Inc., Wallingford CT, 2004.
[27] S.F. Boys, F. Bernardi, Mol. Phys. 19 (1970) 553–566.
[28] Z. Tuce, V. Šoškić, J. Joksimović, Drug Des. Discov. 11 (1994) 251–258.
[29] S. Dukić, S. Kostić-Rajačić, D. Dragović, V. Šoškić, J. Joksimović, J. Pharm. Pharmacol. 49 (1997) 1036–1041.
[30] GraphPad Prism is a biostatistical and curve fitting software packet by GraphPad Software (<http://www.graphpad.com>).